



CHALMERS
UNIVERSITY OF TECHNOLOGY



Impacts of Battery Electric Vehicles on Axle load and Pavement Performance for Swedish Road

Master's thesis in Infrastructure and Environmental Engineering

JINAT TASNIM DRISTY

DEPARTMENT OF ARCHITECTURE AND CIVIL ENGINEERING

CHALMERS UNIVERSITY OF TECHNOLOGY

Gothenburg, Sweden 2026

www.chalmers.se

MASTER'S THESIS 2026

Impacts of Battery Electric Vehicles on Axle load and Pavement Performance for Swedish Road

JINAT TASNIM DRISTY



CHALMERS
UNIVERSITY OF TECHNOLOGY

Department of Architecture and Civil Engineering
Division of Infrastructure and Environmental Engineering
CHALMERS UNIVERSITY OF TECHNOLOGY
Gothenburg, Sweden 2026

Impacts of Battery Electric Vehicles on Axle load and Pavement Performance
for Swedish Road

Jinat Tasnim Dristy

© JINAT TASNIM DRISTY, 2026.

Supervisor: Junze Sun, Department of Architecture and Civil Engineering

Examiner: Kun Gao, Department of Architecture and Civil Engineering

Master's Thesis 2026

Department of Architecture and Civil Engineering

Chalmers University of Technology

SE-412 96 Gothenburg

Telephone +46 31 772 1000

Cover: Descriptive cover

Gothenburg, Sweden 2026

Impacts of Battery Electric Vehicles on Axle load and Pavement Performance for Swedish Road

JINAT TASNIM DRISTY

Department of Architecture and Civil Engineering

Chalmers University of Technology

Abstract

Battery electric vehicles carry battery packs that increase gross vehicle weight and redistribute mass toward the steering axle. Existing flexible pavement standards in Sweden were calibrated to diesel vehicle loading and may be inadequate as heavy electric trucks enter the national freight fleet. This study derives axle loads from manufacturer specifications for a matched pair, the Volvo FM Battery Electric and the Volvo FH 13 diesel, across five goods loading conditions. Load Equivalency Factors and Equivalent Single Axle Loads are calculated using the European 100 kN reference axle. Pavement performance is simulated in ERAPave, calibrated by VTI for Swedish materials and Nordic seasonal conditions, over a 10-year period on a national road cross section in Mölndal, Sweden. Traffic data were obtained from the Trafikverket National Road Database (NVDB). The electric truck imposes a front axle load 1,015 kg heavier than diesel across all loading conditions. The Equivalent Single Axle Load (ESAL) ratio of the electric truck relative to the diesel equivalent peaks at 2.92 under the empty condition and narrows to 1.69 at 90% goods loading, remaining above unity throughout. Fatigue cracking governs the failure sequence, the structural threshold is reached at 4.7 years under electric truck loading versus 8.1 years for diesel. Rut depth is 15% greater after 10 years. Increasing the asphalt-bound layer package by 40 mm reduces the fatigue damage ratio from 1.10 to 0.50, though this structural improvement results in a proportional increase in construction cost. The findings demonstrate that heavy electric trucks will noticeably accelerate pavement deterioration and support a revision of design guidance for designated electric freight corridors in Sweden.

Keywords: Battery Electric Vehicle; Flexible Pavement; Axle Load; Swedish Road Condition

Acknowledgements

Writing this thesis has been quite a journey for me and I would not have made it through without the help of some truly wonderful people.

I am sincerely grateful to my examiner, Kun Gao and my supervisor, Junze Sun for their support throughout this work. My examiner, Kun Gao helped me find the right direction when I was genuinely lost and his guidance gave me the clarity I needed to move forward. My supervisor, Junze Sun was there every single time I came with a problem. His patience and dedication carried me through the hardest parts of this thesis.

On a personal note, I also owe so much to my husband, Sadman Sakib Nobel, who kept believing in me even when I doubted myself. His motivation meant more than words can say. I am equally thankful to my family and friends, who were always there with warmth and encouragement whenever I needed it most.

Thank you all, from the bottom of my heart for making this journey possible for me.

Jinat Tasnim Dristy, Gothenburg, 2026

List of Acronyms

AADT	Annual Average Daily Traffic
AASHTO	American Association of State Highway and Transportation Officials
AC	Asphalt Concrete
BC	Binder Course (pavement layer in ERAPave scenarios)
BEV	Battery Electric Vehicle
ERAPave	Equivalent Road Analysis with Pavement (VTI pavement simulation software)
ESAL	Equivalent Single Axle Load
EU	European Union
EV	Electric Vehicle
FHWA	Federal Highway Administration
GCW	Gross Combination Weight
GHG	Greenhouse Gas
IRI	International Roughness Index
kg	Kilogram
km	Kilometre
KN	Kilonewton
LEF	Load Equivalency Factor
m	Metre
ME	Mechanistic Empirical (pavement design method)
MEPDG	Mechanistic Empirical Pavement Design Guide
mm	Millimetre
PCI	Pavement Condition Index
SEK	Swedish Krona (national currency of Sweden)
VTI	Swedish National Road and Transport Research Institute
WB	Wheelbase
WC	Wearing Course

Table of Contents

CHAPTER 1: INTRODUCTION.....	1
1.1 Research Background	1
1.2 Problem Description	3
1.3 Research purpose and Questions	4
1.4 Delimitations.....	5
CHAPTER 2: LITERATURE REVIEW	6
2.1 Flexible Pavement Damage under Axle Loading	6
2.2 Infrastructure Implications of Battery Electric Trucks	7
2.3 Pavement Deterioration under Electric Truck Loading	8
2.4 Synthesis and Research Positioning.....	9
CHAPTER 3: METHODOLOGY	10
3.1 Research Design.....	10
3.2 Study Area	11
3.3 Vehicle Pair Selection and Specification.....	11
3.4 Axle Load Derivation Method.....	12
3.4.1 Goods load distribution.....	13
3.4.2 Passenger Car Axle Load Derivation.....	14
3.5 Load Equivalency Factor and ESAL Calculation Framework	14
3.6 Pavement Performance Modelling Tool Selection and Application.....	16
CHAPTER 4: AXLE LOAD DISTRIBUTION & SIMULATION RESULTS.....	18

4.1 Vehicle and Trailer Specification	18
4.2 Trailer Axle Load Distribution	18
4.3 LEF and ESAL Results by Loading Scenario.....	19
4.4 Comparative ESAL Summary Across Loading Conditions	21
4.5 Passenger Car Load Equivalency Analysis.....	23
4.6 Pavement Performance Simulation.....	24
4.6.1 ERAPave Pavement Performance Results: Heavy Vehicle.....	25
4.7 Potential Solutions for EV	28
4.7.1 : Increase layer thickness	29
4.8 Cost difference	31
CHAPTER 5: CONCLUSIONS	33
REFERENCES.....	35

List of Tables

Table 3.2-1 : Pavement layer structure	11
Table 3.5-1: Parameters used for LEF and ESAL calculation.....	16
Table 3.6-1: ERAPave simulation scenarios	17
Table 4.1-1: Vehicle and trailer input parameters	18
Table 4.2-1: Trailer axle load distribution for different loading conditions	19
Table 4.3-1: LEF and ESAL Results (Empty Condition)	20
Table 4.3-2: LEF and ESAL Results (50% loaded Condition).....	20
Table 4.3-3: LEF and ESAL Results (70% Loaded Condition)	21
Table 4.3-4: LEF and ESAL Results (90% Loaded Condition)	21
Table 4.5-1: Parameters used in ESAL calculations.....	23
Table 4.5-2: ESAL calculations and ESAL ratio of EV by Diesel	23
Table 4.6-1: Summary of ERAPave Result	28
Table 4.7-1: ERAPave layer thickness input with increased thickness	29
Table 4.8-1: Asphalt mixture cost per mm	31
Table 4.8-2: Unbound granular materials cost per mm	31
Table 4.8-3: Layer by layer cost calculation (base vs proposed structure (per m ²)).....	32

List of Figures

Figure 4.4-1: ESAL Summary across different Loading Conditions	22
Figure 4.4-2: ESAL Ratio: EV versus Diesel across different Loading Conditions	22
Figure 4.6-1: ERAPave layer input showing the pavement structure used in the simulation .	24
Figure 4.6-2: Rutting Estimated under EV Loading	25
Figure 4.6-3: Rutting Estimated under Diesel Vehicle Loading.....	25
Figure 4.6-4: Permanent Deformation by Layer under EV Loading	26
Figure 4.6-5: Permanent Deformation by Layer under Diesel Vehicle Loading.....	26
Figure 4.6-6: Fatigue Cracking Caused by EV Loading.....	27
Figure 4.6-7: Fatigue Cracking Caused by Diesel Vehicle Loading	27
Figure 4.7-1: Permanent Deformation by Layer under EV Loading after Structural Improvement.....	30
Figure 4.7-2: Fatigue Cracking Caused by EV Loading after Structural Improvement.....	30

Chapter 1: Introduction

1.1 Research Background

Road infrastructure is among the most critical and costly assets all over the world that governments maintain. In northern Europe, Sweden maintains one of the most extensive road networks, spanning 98,500 km of national roads and an additional 42,800 km of municipal roads (Hägg, 2025). These roads are fundamental to Swedish daily life and economic activity. They connect cities, carry freight and support industries across the country. Maintaining them is a major public investment. Sweden's proposed National Infrastructure Plan for 2026 to 2037 allocates SEK 315 billion for road maintenance alone (Sweden Proposes the 2026-2037 National Infrastructure Plan – Ministero Degli Affari Esteri e Della Cooperazione Internazionale, n.d.). By 2023, more than 25% of the national road network was classified as poor condition and 11% as very poor, a worsening trend from previous years (Hägg, 2025). The maintenance backlog grew from SEK 16.5 billion in 2022 to SEK 19.1 billion in 2023 and is projected to reach SEK 46 billion by 2033, if current funding levels continue. Trafikverket has already been forced to reduce speed limits on 1,200 km of national roads due to deteriorating surfaces. At the municipal level, a national survey of 147 Swedish municipalities found that potholes, surface unevenness and alligator cracking are the most reported distresses. Heavy traffic and pavement ageing were identified as the leading causes of this deterioration (Afridi et al., 2023). These conditions describe a road network under sustained and growing pressure.

Into this context of ageing roads and growing maintenance pressure, a major transformation of the vehicle fleet is now under way. Sweden has legally binding climate targets that require a 70% reduction in domestic transport sector greenhouse gas emissions by 2030 compared to 2010 levels (Sweden's Climate Act and Climate Policy Framework, n.d.). Transport accounts for approximately 31% of Sweden's total national GHG emissions, making it the country's largest emitting sector (Sweden's Climate Act and Climate Policy Framework, n.d.). To meet these targets, battery electric vehicles have become the central policy instrument. Sweden is one of the leading countries in Europe for adoption. Battery electric vehicles accounted for 35% of all new passenger car registrations in Sweden in 2024 (Sweden: 35% BEV Market Share in 2024 | European Alternative Fuels Observatory, n.d.). In the heavy truck segment,

electric models captured 6.5% of new registrations in 2024, rising to 8.9% in January 2025, representing a 15.8% year on year increase (Sweden's EV Market in January 2025: 14.4% YoY Increase | European Alternative Fuels Observatory, n.d.). By 2025, nearly 19% of all newly registered heavy trucks in Sweden were battery electric, reaching a total electric heavy truck fleet of 1,634 vehicles (Sweden Reaches 15% EV Car Fleet in 2025 | European Alternative Fuels Observatory, n.d.). Sweden is also home to Volvo Trucks and Scania, two of the world's largest truck manufacturers. Volvo Trucks held a 47% share of the European heavy electric truck market in 2024 and identified Sweden as one of its five most important markets for electric trucks (Volvo Trucks, 2025). The shift is no longer a forecast. It is a measurable, accelerating reality on Swedish roads.

Battery electric trucks and passenger cars differ from their conventional counterparts across several operationally significant dimensions. They produce zero tailpipe emissions at the point of use, directly contributing to national GHG reduction targets. Their drivetrain architecture eliminates the internal combustion engine, reducing certain maintenance requirements for vehicle operators while introducing new dependencies on charging infrastructure and battery replacement cycles (Engholm et al., 2025). In terms of vehicle dynamics, electric drivetrains deliver higher instantaneous torque compared to diesel engines, altering acceleration and braking load profiles. Most consequentially for road infrastructure, battery electric vehicles carry large battery packs that increase gross vehicle weight relative to equivalent conventional models. A long haul heavy electric truck can carry a battery pack exceeding 3,600 kg and a battery electric passenger car is typically 200 to 500 kg heavier than its petrol equivalent (Mattinzioli et al., 2023). This additional mass is distributed unevenly across the axle groups, depending on battery placement within the chassis. The resulting changes in per axle loading have direct implications for flexible pavement performance, implications that existing design standards, calibrated to conventional diesel traffic, were not developed to accommodate.

These weight differences have direct structural implications for road pavements. Battery electric trucks alter axle load magnitude and distribution relative to the diesel vehicles they replace. Sweden's Nordic climate, characterised by spring thaw cycles that temporarily reduce subgrade bearing capacity, further amplifies load induced structural stress beyond what temperate climate design standards account for (Afridi et al., 2023). Whether the design standards, condition classification thresholds and maintenance frameworks currently governing the Swedish road network remain valid under accelerating BEV fleet penetration is

therefore an open engineering question and one with significant infrastructure cost implications. Section 1.2 defines this problem in specific technical terms.

1.2 Problem Description

The shift toward battery electric vehicles challenges current roads of Sweden, which was made mainly for the diesel vehicle. Electric vehicles carry battery packs that increase gross vehicle weight and critically, alter how that weight is distributed across individual axles. Given the fourth power relationship between axle load and pavement damage, even modest increases in axle load at the steering or drive axle can substantially accelerate both fatigue and rutting accumulation.

Pavement damage under repeated traffic loading manifests through two principal mechanisms. The first is fatigue cracking, which initiates as tensile strain at the bottom of the asphalt bound layer and propagates upward through repeated loading cycles until it reaches the surface as alligator cracking. The second is permanent deformation or rutting, which accumulates progressively in the wheel tracks under compressive loads. Both mechanisms are evaluated using the Load Equivalency Factor (LEF) framework, which converts axle loads into equivalent passes of a standard European 100 kN single axle and the Equivalent Single Axle Load (ESAL), which aggregates those passes over a design life. Together, these form the foundational inputs for pavement damage assessment. Pavement condition is then classified through methods such as the Pavement Condition Index (PCI) and the International Roughness Index (IRI), which translate cumulative structural damage into measurable surface deterioration. These classification systems are calibrated to the vehicle loading assumptions that prevailed when existing pavements were designed. This creates a need to reevaluate whether current LEF and ESAL values, pavement design standards and condition classification thresholds remain valid for roads that will increasingly carry electric rather than diesel traffic.

The current state of the quantitative evidence base has not yet fully addressed this need. A systematic review of 55 studies across the EV pavement interaction field identified the effect of electric vehicles on pavement degradation as one of the most critical unresolved knowledge gaps in transportation engineering (Mattinzioli et al., 2023). The majority of quantitative studies to date have been conducted in the United States, drawing on American vehicle classifications, US pavement design standards and American climate data (Fares et al., 2024;

John Harvey, 2020; Zhou et al., 2024), which limits the transferability of their findings to European and Swedish conditions.

Regarding load equivalency data, studies that have calculated LEFs for battery electric trucks have generally relied on hypothetical vehicle configurations (Gkyrtis, 2025) or American vehicle classes such as the Tesla Semi and FHWA Class 9 trucks (Fares et al., 2024). Axle load data derived from the manufacturer specifications of a commercially available European heavy electric truck, used to calculate LEF and ESAL values in direct comparison to a diesel equivalent under European axle load conventions, has not been reported in the literature. A reliable pavement damage comparison for the European context therefore requires this foundational data to be established.

Regarding pavement performance modelling, mechanistic empirical simulations published to date have been calibrated to US structural and climate inputs. Modelling of how a representative Swedish flexible pavement progresses toward its critical thresholds for fatigue cracking and rutting under electric vehicle traffic, accounting for Swedish pavement layers and Nordic seasonal climate behaviour, has not been reported. Sweden's spring thaw temporarily reduces the load bearing capacity of the pavement structure, making each passing axle disproportionately more damaging than under temperate conditions (Afridi et al., 2025). This seasonal amplification is a structurally significant dimension of the problem for Swedish roads that has not yet been quantified under electric truck loading. Trafikverket and Swedish municipalities are beginning to plan for a future with substantially more electric heavy vehicles and would benefit from quantitative evidence on the additional stress these vehicles place on road infrastructure and the design adjustments that may be required. This study is positioned to contribute that evidence.

1.3 Research purpose and Questions

Given the accelerating adoption of battery electric vehicles in Sweden, the nonlinear relationship between axle load and pavement damage and the limited availability of quantitative pavement damage analysis derived from European heavy electric vehicle specifications and Nordic climate conditions, this study addresses a specific and practically relevant knowledge gap. Its purpose is to determine how battery electric heavy trucks and battery electric passenger cars differ from their conventional counterparts in axle loading

characteristics, to quantify what those differences mean for the performance and service life of Swedish flexible pavements and to identify what pavement design adaptations may be required in response. Depending on this purpose this research will answer the three research question stated below-

RQ1: How does weight distribution differ between battery electric and conventional heavy duty trucks?

RQ2: How do differences in axle loading influence pavement damage?

RQ3: What are the potential pavement design adaptations that could mitigate the increased load-induced damage caused by battery electric trucks on flexible pavements?

1.4 Delimitations

This study is bounded by a set of scope decisions made to maintain analytical clarity and focus.

The following delimitations apply:

- The analysis is confined to flexible asphalt pavements. Rigid concrete pavements fall outside the scope of this study.
- The vehicle analysis is based on a matched pair approach. One battery electric heavy truck is paired with a diesel equivalent and one battery electric passenger car is paired with a conventional petrol counterpart, both from the same manufacturer. This approach isolates electrification as the primary variable while maintaining comparability across other vehicle parameters.
- The heavy truck and passenger car pairs are analyzed separately. Combined or mixed fleet effects are therefore not captured in this study
- Design adaptations discussed in response to RQ3 are indicative rather than detailed engineering specifications and represent directions for future research.

Chapter 2: Literature Review

This chapter builds the foundation for the analysis that follows. It moves from the structural composition of flexible pavements and how axle loads damage flexible pavements, through what is known about how battery electric trucks alter those loads, to the pavement performance outcomes that have been observed in existing studies. The chapter closes by identifying the specific gaps this thesis is positioned to fill.

2.1 Flexible Pavement Damage under Axle Loading

A flexible asphalt pavement consists of multiple bound and unbound layers, a wearing course and binder course of compacted asphalt concrete, an unbound granular base, an unbound subbase, and a subgrade. Each layer serves a structural function, distributing the load applied at the surface progressively downward so that stress intensities reduce with depth. When a vehicle wheel passes over the pavement surface, the tyre contact force is transmitted through these layers as a combination of vertical compressive stress and horizontal tensile strain. The magnitude of both depends directly on the axle load and the stiffness of each layer. Heavier axle loads produce larger tensile strains at the base of the asphalt bound layers and larger compressive stresses at the subgrade. It is these stress and strain responses, repeated across millions of vehicles passes over a design life, that drive the two principal structural failure modes in flexible pavements.

Flexible asphalt pavements fail primarily through two load driven mechanisms. The first is fatigue cracking. Repeated loading creates tensile strain at the bottom of the asphalt layer. Over time, these strains cause cracks that grow upward and eventually appear at the surface as alligator cracking (Gkyrtis, 2025). The second failure mode is rutting, which is the permanent deformation that accumulates in the wheel tracks under compressive loads. Both distresses are nonlinear. Damage scales approximately with the fourth power of the axle load. A 10% increase in axle load causes roughly 46% more pavement wear per pass and doubling the axle load multiplies damage by sixteen (Chua & Nepal, 2025).

This nonlinearity is why the Load Equivalency Factor (LEF) exists. It converts any axle load into an equivalent number of passes by a standard reference axle. These values are accumulated across all vehicles passes over a design life to produce the Equivalent Single Axle Load

(ESAL), which is the primary traffic input to pavement design. How those ESALs translate into predicted road deterioration depends on the design method applied.

Two methods appear repeatedly in the literature on electric vehicle pavement impacts. The AASHTO 1993 empirical method derives a Structural Number from ESAL inputs but cannot account for seasonal climate variation, material specific asphalt behaviour or axle specific load effects. Fares et al. (2024) showed that this method over designs pavements in heavy duty scenarios because it cannot distinguish how different load configurations stress individual pavement layers differently. The Mechanistic-Empirical (ME) method is more accurate. It computes actual tensile and compressive strains within each layer and uses calibrated transfer functions to predict cracking and rutting over time. Critically, it responds to climate inputs. In Sweden, spring thaw temporarily reduces the load bearing capacity of the pavement structure, making each passing axle disproportionately more damaging (Afridi et al., 2023). The ME method can capture this, the AASHTO 1993 method cannot.

2.2 Infrastructure Implications of Battery Electric Trucks

The key difference between a battery electric truck and a diesel truck, from a road infrastructure perspective, is not just total weight but how that weight is distributed across the axles. A diesel truck carries its engine and drivetrain mass concentrated toward the rear, which typically places 25 to 40% of the vehicle weight on the steering axle and 60 to 75% on the rear drive axles (Fares et al., 2024). A battery electric truck changes this balance. The battery pack can weigh up to 3,600 kg and is usually mounted low in the chassis to keep the centre of gravity stable. Depending on where it sits, it shifts load toward the front of the vehicle and increases the stress on the steering axle (Chua & Nepal, 2025). It is worth noting that the higher torque of electric drivetrains, which is often raised as a concern, turns out to be less important than battery location in determining the vertical forces the vehicle places on the road surface.

This matters enormously because of the fourth power law described in Section 2.1. When the battery is placed at the steering axle, fatigue damage can increase by as much as 185 to 201% compared to a diesel truck of equivalent total weight. When the same battery mass is placed at the rear driving axles instead, the damage is almost identical to diesel, within approximately 5%. A distributed placement across all tractor axles lands in between, at around 34 to 37% more damage (Gkyrtis, 2025). This means battery placement is not merely a vehicle design

choice. It is an infrastructure decision and a consequential one. The difference between the best and worst placement scenario is a factor of more than five in fatigue damage.

2.3 Pavement Deterioration under Electric Truck Loading

Understanding how individual axle loads change is necessary, but it is not enough on its own. The more important question for road planning is what those changed loads mean for how quickly pavements deteriorate. The evidence on this is consistent, even if the specific numbers vary by context.

When electric truck penetration increases in the traffic mix, pavement distress accelerates across all failure modes. At full electric truck replacement, fatigue cracking increases by approximately 29%, rutting by 5% and surface roughness by 26% compared to an equivalent all diesel traffic scenario (Zhou et al., 2024). The roughness increases matters beyond comfort. A rougher road increases the energy consumption of electric trucks, which means pavement deterioration and vehicle operating costs are connected in a feedback loop that does not exist in the same way for diesel vehicles.

The rate at which this deterioration sets in is also faster than simple proportional scaling might suggest. Even a partial replacement of diesel trucks, as low as 12.5% of the fleet, is enough to trigger premature pavement failure on roads that were adequately designed for the existing diesel load (Fares et al., 2024). Replacing half the diesel fleet reduces the expected service life from 20 years to under 10. This is not a gradual degradation. It is a step change that existing pavement design frameworks, calibrated to diesel loading, are not equipped to predict. The ME method captures this behaviour; the AASHTO 1993 empirical method does not, which is a further reason why the ME approach is the appropriate tool for this kind of assessment.

The vulnerability is not evenly distributed across road types. Local and municipal roads are structurally thinner than national highways and were not designed to carry heavy freight loads. A 1 tonne increase in steer axle mass reduces pavement life on local roads by 31 to 49%, compared to only 20.9% on national highways (Chua & Nepal, 2025). This asymmetry is important for Swedish conditions, where electric trucks will travel not only on highways but also on the thinner municipal streets that connect distribution centres to delivery points.

There is also a policy dimension that the technical literature tends to understate. Weight exemptions are commonly granted to electric and alternative fuel trucks to offset the mass of their battery or fuel system. These exemptions shorten pavement service life substantially, yet this infrastructure cost is rarely reflected in the policy frameworks that grant them (John Harvey, 2020). Vehicle weight policy and road maintenance planning are currently developed through separate processes, without the quantitative connection needed to make informed trade offs between them.

2.4 Synthesis and Research Positioning

The existing literature establishes a coherent mechanistic foundation. The fourth power axle load relationship combined with battery induced front axle overloading, produces nonlinear damage outcomes that are highly sensitive to battery placement. The mechanistic empirical method emerges as the most appropriate analytical framework, particularly under seasonal climate conditions where structural capacity fluctuates.

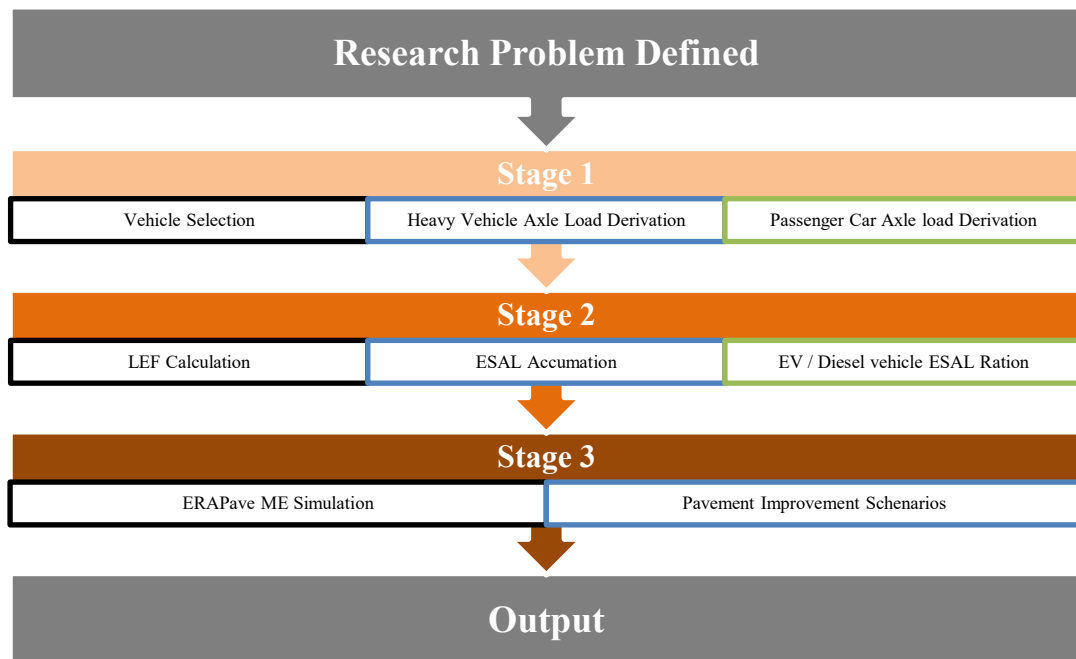
However, the reviewed studies share a common geographic and regulatory boundary. Load equivalency analyses draw predominantly on American vehicle classifications and weight regulations. Pavement performance simulations are calibrated to US structural and climate inputs. Design guidance is framed within US and Australian regulatory contexts. Consequently, their direct transferability to European vehicle configurations, Nordic seasonal behaviour and Swedish design standards remains limited. Quantitative pavement damage analysis derived from commercially available European electric truck specifications under Nordic climate conditions has not been established. This thesis addresses that gap directly through the three research questions stated in Chapter 1.

Chapter 3: Methodology

This chapter presents the methodological framework that underpins the analytical work reported in Chapter 4. The chapter is organised into six sections corresponding to the six methodological components: research design, study area, vehicle selection, axle load derivation, load equivalency and traffic damage calculation and pavement performance modelling. For each component, the rationale is stated explicitly, why a particular method was chosen, why it is the most appropriate approach for the Swedish context and how it was applied.

3.1 Research Design

The study addresses three research questions that operate at successive levels of analysis: axle load characterisation, pavement damage quantification and design adaptation. This progression demands a sequential, quantitative methodology in which each stage builds directly on the outputs of the preceding stage. The research therefore follows a three-stage analytical workflow, as illustrated below-



3.2 Study Area

The study road is a section of Swedish national road located in the municipality of Mölndal, Västra Götaland County, identified using the Trafikverket National Road Database (NVDB) and the associated spatial viewer (nvdbaparta.trafikverket.se). Mölndal was selected for several reasons. Firstly, the section carries a measured Annual Average Daily Traffic (AADT) of 1,601 heavy vehicle movements per day. This places it within the intermediate traffic volume range typical of Swedish national roads outside major urban arterials, making it representative rather than anomalous for generalisation. Moreover, Mölndal lies adjacent to the Port of Gothenburg freight corridor, which is the highest volume goods transport route in Scandinavia. It is therefore a realistic early deployment corridor for battery electric heavy trucks, which makes it directly relevant to the scenario this study is intended to inform. Additionally, the road cross section available for Mölndal matches the structural profile used in the ERAPave VTI calibration dataset for Swedish national road conditions (Trafikverket, 2020), ensuring internal consistency between the study road and the modelling tool. The pavement structure used in all ERAPave simulations is the standard Swedish national road cross section from the ERAPave software manual (Ahmed & Erlingsson, n.d.) presented in Table 3.1. This cross section is held constant for both EV and Diesel vehicle simulation runs, so that performance differences are attributable solely to traffic loading variation.

Table 3.2-1 : Pavement layer structure

Layer	Material designation	Bitumen grade	Thickness (mm)	Layer type
1	ABT11 -wearing course	70/100	40	Asphalt bound
2	ABb16 -binder course	50/70	50	Asphalt bound
3	AG22 -AC road base	160/220	65	Asphalt bound
4	GW-CR -unbound base	-	80	Granular unbound
5	GW-CR -unbound subbase	-	420	Granular unbound

3.3 Vehicle Pair Selection and Specification

The central methodological challenge is isolating electrification as the variable of interest. A comparison between two vehicles that differ in axle configuration, wheelbase, gross

combination weight (GCW) rating or body type would confound the effect of electrification with those of other design differences. A matched pair approach is therefore applied: the electric vehicle and its conventional counterpart are drawn from the same manufacturer and share the same fundamental architecture.

The primary heavy vehicle pair consists of the Volvo FM Battery Electric (Volvo FM EV) and the Volvo FH 13 4×2 tractor (Volvo FH diesel). Both vehicles are manufactured by Volvo Trucks, share a 4×2 axle configuration (single steering axle, single rear tandem drive axle), and operate under the same GCW limit under Swedish and European Regulation (EU) 2015/719. This design ensures that electrification is the sole independent variable.

The selection of Volvo vehicles is further justified by market relevance. Volvo Trucks held a 47% share of the European heavy electric truck market in 2024 and identified Sweden as one of its five priority markets for electric truck deployment (Volvo Trucks, 2025). The Volvo FM EV and its diesel counterpart are among the most common vehicle types that Swedish road infrastructure must accommodate as fleet electrification accelerates.

A secondary analysis compares a battery electric passenger car with a conventional petrol equivalent. The same matched pair logic applies: both vehicles are drawn from the same model range. The BEV car is heavier than its petrol counterpart owing to the battery pack, increasing both front and rear axle loads. While individual passenger cars generate negligible pavement damage relative to heavy trucks, passenger cars account for 82% of total vehicle kilometres in Sweden (Statistics Sweden, 2023). Fleet wide electrification therefore produces a cumulative loading increment across millions of daily passes that warrants quantification.

3.4 Axle Load Derivation Method

Manufacturer specification sheets report gross vehicle weight and axle capacity limits, not the actual loads imposed under a given loading condition. Actual per axle loads depend on how the combined weight of the tractor, trailer and cargo is distributed across the axle groups of the combination. This distribution is governed by trailer geometry and cargo centre of gravity location. Static moment equilibrium provides the analytical framework, the sum of moments about the trailer bogie centre equals zero, yielding the kingpin connection force, F_c , the vertical

load transferred from the trailer to the tractor at the fifth wheel coupling. The per axle loads then follow from a free body analysis of the tractor.

This approach is the standard analytical method adopted in vehicle load calculation studies in the pavement engineering literature (Gkyrtis, 2025; John Harvey, 2020) and requires no additional instrumentation or field measurement. It produces reproducible, specification consistent results directly comparable to the regulatory axle load limits under which Swedish roads are designed.

3.4.1 Goods load distribution

Five loading conditions are evaluated in this analysis: empty, 50%, 70%, 90% and fully loaded. The empty and fully loaded conditions represent the absolute operational bounds of the vehicle combination. Payload fractions below 50% of maximum capacity correspond primarily to repositioning runs and partial backhaul operations. Between 30% and 50% of commercial vehicle trips in Europe are estimated to run empty. Laden trips in operational freight service consistently exceed 50% payload utilisation (Meßmer et al., 2025). Sub-50% loading conditions are therefore not representative of the dominant freight operating regime on Swedish roads. The 50% goods loading condition is adopted as the lower bound of the intermediate payload range.

From 50% upward, increments of 20 percentage points are applied, yielding 70% and 90% loading conditions. This step size provides sufficient resolution to capture the nonlinear variation in per axle load with increasing payload. The 90% condition serves as the upper bound for the incremental load.

Goods are assumed to be uniformly distributed across the full trailer floor, placing the cargo centre of gravity (d_{cg}) at the geometric midpoint. This is the standard assumption for homogeneous palletised freight. The moment balance about the bogie centre gives:

$$F_C = \frac{(W_{trailer} \times d_{bogie} - d_{cg})}{L_{kingpin-bogie}} \quad (1)$$

where, $W_{trailer}$ is the total trailer weight including goods; $(d_{bogie} - dcg)$ is the horizontal distance from bogie centre to the cargo dcg; and $L_{kingpin-bogie}$ is the kingpin to bogie distance. The front axle of both vehicle is assumed fixed in all cases. In a tractor semi trailer system, trailer cargo transfers load to the tractor through the fifth wheel at the rear of the tractor frame, while any forward transfer to the steering axle through chassis bending is negligible and not considered in this static analysis. The remaining trailer weight (total minus F_c) distributes equally across the three trailer axles (tridem group). The tractor rear axle load is then F_c plus the tractor's own unloaded rear axle contribution.

3.4.2 Passenger Car Axle Load Derivation

For the passenger car pair, a static 60/40 front to rear axle load split is applied to the gross vehicle weight. This is the standard engineering approximation for a standard passenger car with a front engine layout (Mattinzioli et al., 2023). The BEV car's additional battery mass is distributed using the same 60/40 ratio, a conservative assumption, given that battery packs are typically mounted low and centrally in the chassis. The empty (kerb weight) condition is evaluated.

3.5 Load Equivalency Factor and ESAL Calculation Framework

Raw axle loads in kilonewtons are not directly useful for pavement design comparison because pavement damage does not scale linearly with load. The fourth power relationship established through the AASHO Road Test (Highway Research Board, 1962) and extensively validated in subsequent literature means that a 10% increase in axle load increases damage per pass by approximately 46% and doubling the axle load multiplies damage by sixteen (Chua & Nepal, 2025). The LEF framework converts this nonlinear relationship into a dimensionless equivalency factor. ESAL then aggregates those factors over traffic volume and design life to produce a single traffic damage input for pavement design.

Why LEF and ESAL rather than direct mechanistic input? In the ME modelling stage (Section 3.6), ERAPave accepts ESAL as its traffic input. LEF and ESAL therefore serve a dual purpose, they provide a standardised, regulatory consistent comparison metric between the EV and diesel vehicles and they form the direct input to the simulation tool. This is consistent with the approach adopted in comparable European studies (Chua & Nepal, 2025; Mattinzioli et al., 2023).

The reference axle adopted is the standard European single axle of 100 kN (approximately 10 tonnes), consistent with Swedish and European pavement design practice. This differs from the 80 kN (18 kip) reference used in American studies. The European reference is adopted because it reflects the regulatory and design framework within which Swedish roads are built and maintained and because using the American reference would produce LEF values that are not directly comparable to Swedish design standards.

The LEF formula applied to each axle group is:

$$LEF = a \times \left(\frac{P}{100}\right)^4 \quad (2)$$

where P is the axle load in kilonewtons; and a is the axle type factor accounting for multi axle load sharing. For single axles, a = 1.0. For tridem axle groups, a = 0.05 (AASHTO, 1993). The tridem factor reflects the substantially reduced damage per unit of total load when load is distributed across three closely spaced axles.

The ESAL for each vehicle type and loading scenario is calculated as:

$$ESAL = AADT \times LEF_{total} \times L \times D \times 365 \times GF \quad (3)$$

where the traffic growth factor GF over design horizon Y years is:

$$GF = [(1 + r)^Y - 1] / r \quad (4)$$

Table 3.5-1 lists all parameter values with their sources. The AADT of 1,601 is drawn from the Trafikverket NVDB for the Mölndal study section. The lane distribution factor of 0.80 reflects a two lane road in each direction, where approximately 80% of heavy vehicles use the outer lane (AASHTO, 1993). The 1.4% annual growth rate is based on Wikström (2024) for heavy trucks and 15% for passenger car (European Alternative Fuels Observatory, n.d.). The 10 year design horizon is consistent with Swedish road maintenance planning practice (Trafikverket, 2020).

Table 3.5-1: Parameters used for LEF and ESAL calculation

Parameter	Value	Source
AADT	1,601	Trafikverket NVDB (https://nvdbpakarta.trafikverket.se/map)
Lane distribution factor (L)	0.80	AASHTO (1993), two lanes each direction
Directional distribution (D)	1.00	Single-direction analysis
Annual growth rate Heavy trucks (r)	1.4%	Wikström (2024)
Annual growth rate Passenger cars, (r)	15%	(European Alternative Fuels Observatory, n.d.)
Design horizon (Y)	10 years	Swedish road maintenance planning standard
Growth factor (GF)	10.654	Computed from Equation 3.4
Axle type factor -single axle (a)	1.000	AASHTO (1993)
Axle type factor-tridem group (a)	0.05	AASHTO (1993)
Reference axle load	100 kN	European standard; Swedish design practice

3.6 Pavement Performance Modelling Tool Selection and Application

The Mechanistic Empirical modelling framework was selected as the pavement performance evaluation tool for this study. As established in the literature review (Section 2.1), the AASHTO 1993 empirical method treats total ESAL as the sole traffic descriptor. It cannot differentiate how individual axle configurations distribute stress within the pavement structure. Fares et al. (2024) demonstrated that this leads to over design in heavy duty scenarios, because the method cannot detect the disproportionate damage caused by front axle overloading. It also provides no mechanism for seasonal capacity variation, a fundamental limitation for Nordic Road conditions. The ME approach resolves both limitations.

For ME simulation ERAPave software is used. ERAPave (Equivalent Road Analysis with Pavement) is a mechanistic empirical pavement design and performance simulation tool developed and maintained by VTI, the Swedish National Road and Transport Research Institute. It is calibrated for Swedish pavement materials, layer configurations and climate conditions using field monitoring data from the Swedish road network (Trafikverket, 2020).

All ERAPave simulations use the pavement cross section and a 10year modelling period. The traffic input is the ESAL value for the loading condition under analysis. Two baseline simulations establish the comparative reference: one with the EV ESAL as input and one with the diesel ESAL, both at the 90% goods loading condition.

Following the baseline simulations, three structural improvement scenarios are evaluated all, using the EV ESAL as input, since the adaptations are designed to address the more demanding loading condition. Table 3.6-1 summarises all scenarios.

Table 3.6-1: ERAPave simulation scenarios

Scenario	Description	Traffic input	Failure mode targeted
Baseline EV	Standard cross section, EV ESAL	EV, (90% loaded condition)	
Baseline Diesel	Standard cross section, diesel ESAL	Diesel, (90% loaded condition)	
Improved Scenario	Increased AC thickness: +15 mm WC, +15 mm BC, +10 mm base	EV, (90% loaded condition)	Fatigue cracking

Chapter 4: Axle Load Distribution & Simulation Results

4.1 Vehicle and Trailer Specification

The load calculations are based on the manufacturer specifications of the Volvo FM Battery Electric and Volvo FH 13 4x2 Tractor (Diesel) operating with a standard semi trailer. The front axle load of the EV tractor is fixed at 6,010 kg across all loading conditions, reflecting the location of the battery pack at the front of the chassis. The diesel front axle is fixed at 4,995 kg. In a tractor semi trailer system, trailer cargo transfers load to the tractor through the fifth wheel at the rear of the tractor frame, while any forward transfer to the steering axle through chassis bending is negligible and not considered in this static analysis. The trailer geometry and vehicle combination parameters used throughout are summarised in Table 4.1.

Table 4.1-1: Vehicle and trailer input parameters

Parameter	Value	Unit
Trailer length	13.62	m
Trailer width	2.48	m
Trailer height	2.7	m
Wheelbase (WB)	7,700	mm
Kingpin distance	1,690	mm
Trailer weight (empty)	6,335	kg
Max goods weight (EV)	23,800	kg

With the EV tractor weighing 9,865 kg and the empty trailer 6,335 kg, the maximum allowable goods weight for the EV combination is 23,800 kg. This value defines the fully loaded condition.

4.2 Trailer Axle Load Distribution

For different loaded condition, goods are assumed to be distributed evenly across the full trailer floor, placing the centre of gravity of the cargo at the geometric centre of the trailer. A moment balance about the bogie centre is used to calculate the connection force F_c transferred from the trailer to the tractor rear axle. The remaining trailer load is distributed equally across the three

trailer axles considered as one group. Table 4.2-1 presents the results for different loading conditions.

Table 4.2-1: Trailer axle load distribution for different loading conditions

Goods %	Trailer weight(kg)	Fc (kg)	Trailer Axle load(kg)	Rear Axle Load (EV)(kg)	Rear Axle (Diesel)(kg)
Empty	6335	2123	4212	5978	3968
50	18235	6110	12125	9965	7970
70	22995	7705	15290	11560	9565
90	27755	9300	18455	13155	11160
Fully loaded	30135	10097	20038	13952	11942

In practice, freight vehicles rarely operate at full rated capacity due to cargo variability and weight distribution constraints. The fully loaded condition is therefore excluded from the further calculation.

4.3 LEF and ESAL Results by Loading Scenario

This section presents the LEF and ESAL results calculated for the Volvo FM EV and Volvo FH 13 diesel across five loading conditions: empty, 50% 70% and 90% goods loading. For each condition the axle loads derived in Section 4.2 are converted into Load Equivalency Factors using the AASHTO fourth power formula and then aggregated into Equivalent Single Axle Loads over the 10 years design horizon. The results show how the fixed battery mass on the EV front axle elevates damage equivalency across all loading conditions and how the EV/diesel ESAL ratio varies with payload.

Empty Condition

Table 4.3-1: LEF and ESAL Results (Empty Condition)

Axle	EV Load (kg)	EV Load (kN)	Diesel Load (kg)	Diesel Load (kN)	LEF Diesel	LEF EV
Front	6010	58.958	4995	49.001	0.0577	0.1208
Rear	5978	58.641	3983	39.070	0.0233	0.1182
Trailer	4212	41.323	4212	41.323	0.001458	0.001458
LEF Total					0.0824	0.2405
ESAL					410463.25	1198038.84

50% Goods Loading

Table 4.3-2: LEF and ESAL Results (50% loaded Condition)

<i>Axle</i>	<i>EV Load (kg)</i>	<i>EV Load (kN)</i>	<i>Diesel Load (kg)</i>	<i>Diesel Load (kN)</i>	<i>LEF Diesel</i>	<i>LEF EV</i>
Front	6010	58.96	4995	49.00	0.06	0.12
Rear	9965	97.76	7970	78.18	0.37	0.91
Trailer	12125	118.95	12125	118.95	0.10	0.10
LEF Total					0.53	1.13
ESAL					2646811.21	5648752.12

70% Goods Loading

Table 4.3-3: LEF and ESAL Results (70% Loaded Condition)

Axle	EV Load (kg)	EV Load (kN)	Diesel Load (kg)	Diesel Load (kN)	LEF Diesel	LEF EV
Front	6010	58.96	4995	49.00	0.06	0.12
Rear	11560	113.40	9565	93.83	0.78	1.65
Trailer	15290	150.00	15290	150.00	0.25	0.25
LEF Total					1.09	2.03
ESAL					5408552.35	10099489.73

90% Goods Loading

Table 4.3-4: LEF and ESAL Results (90% Loaded Condition)

Axle	EV Load (kg)	EV Load (kN)	Diesel Load (kg)	Diesel Load (kN)	LEF Diesel	LEF EV
Front	6010	58.96	4995	49.00	0.06	0.12
Rear	13155	129.05	11160	109.48	1.44	2.77
Trailer	18455	181.05	18455	181.05	0.54	0.54
LEF Total					2.03	3.43
ESAL					10117274.71	17090615.32

4.4 Comparative ESAL Summary Across Loading Conditions

The results presented in Section 4.3 show that EV ESALs are consistently and substantially higher than diesel across all conditions. The highest absolute ESAL values occur at 90% loading condition, reflecting that the 90% loading condition, rear axle is the dominant damage

source. At other loading condition total ESAL values are lower in magnitude, but the relative gap remains large. Figure 4.4-1 presents the ESAL summary across different loading conditions.

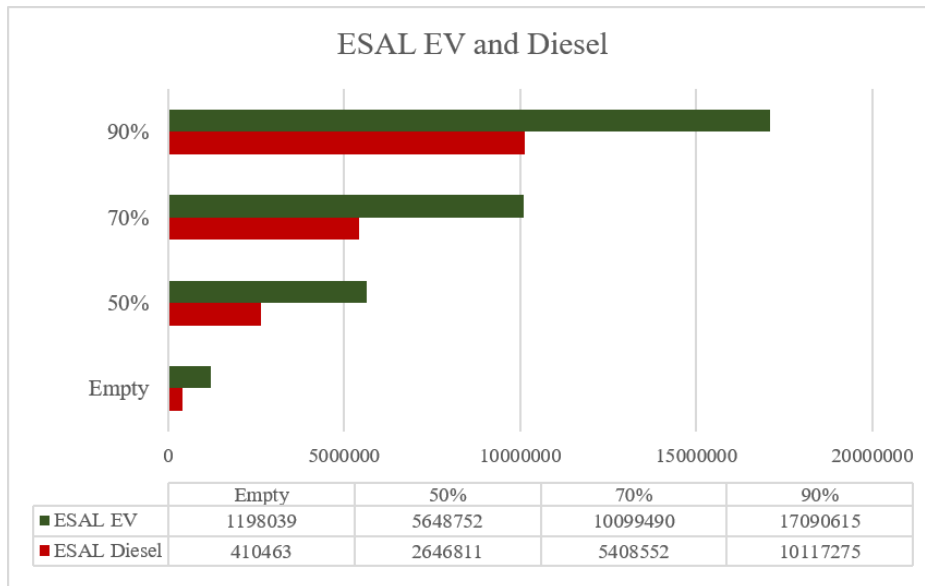


Figure 4.4-1: ESAL Summary across different Loading Conditions

From the summary result it is visible that the ratio is not constant it varies significantly with loading condition which is the most important finding of this section. The ratio peaks at 2.92 under the empty condition, where the EV generates approximately three times more pavement damage than the diesel. As payload increases, the diesel rear axle load also rises, gradually narrowing the damage gap. At 90% loading, the ratio drops to 1.69, but still remains above 1, indicating that the EV always causes more damage regardless of loading level. The EV/Diesel ESAL ratio is presented in Figure 4.4-2.

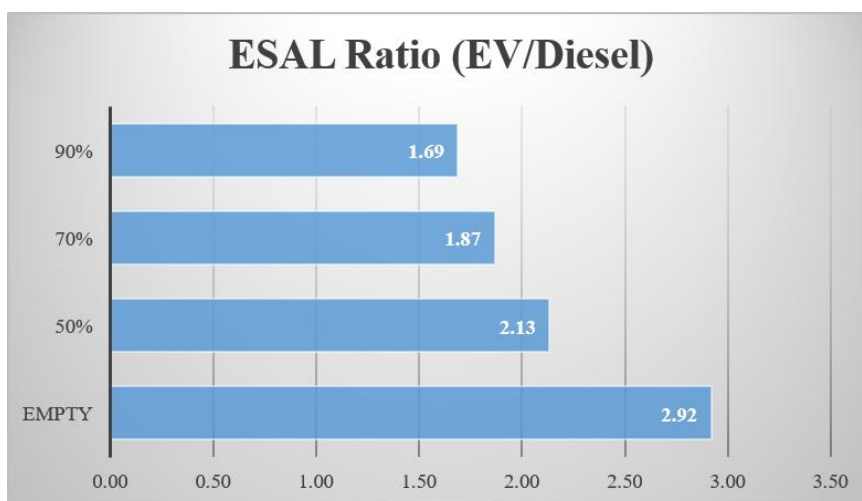


Figure 4.4-2: ESAL Ratio: EV versus Diesel across different Loading Conditions

4.5 Passenger Car Load Equivalency Analysis

A secondary analysis was conducted for a battery electric car paired with a conventional petrol car. Passenger cars represent 82% of total vehicle km in Sweden (Statistics Sweden 2023). An annual EV growth rate of 15% was applied. Table 4.5-1 shows the parameter used in ESAL calculation and Table 4.5-2 presents the calculation.

Table 4.5-1: Parameters used in ESAL calculations

Parameter	Value	Source / Note
AADT (Total)	16001	Trafikverket (nvdbaparta)
AADT (Passenger cars) (82% of total AADT)	13120	(Statistics Sweden, 2023)
Annual Growth Rate (r)	15 %	(European Alternative Fuels Observatory n.d.) Applied equally to EV and Diesel
Growth Factor (GF) -10 years	10.654	$GF = \frac{[(1 + r)^Y - 1]}{r}$

Empty Condition

Table 4.5-2: ESAL calculations and ESAL ratio of EV by Diesel

Axle	EV Load (kg)	EV Load (kN)	Diesel Load (kg)	Diesel Load (kN)	LEF Diesel	LEF EV
Front	1020	10.006	1013	9.936	0.0000974	0.0001002
Rear	1020	10.006	675	6.624	0.0000192	0.0001002
LEF Total					0.00012	0.00020
ESAL					4501.26	7733.63
Ratio (EV/Diesel)					1.72	1.72

The EV car generates 1.7 times more ESALs than its diesel counterpart. Although the absolute damage is less compared to heavy trucks, however the high daily volume means the differential accumulates across millions of passes increasingly relevant as Sweden's passenger car fleet electrifies.

4.6 Pavement Performance Simulation

Simulations were run in ERAPave (calibrated by VTI for Swedish conditions six Nordic climate seasons). The pavement layer structure used as input in ERAPave is presented in Figure 4.6-1. It consists of five layers including three asphalt bound layers and two unbound granular layers. The subgrade is classified as 4e-Lera, representing a clay subgrade typical of Swedish national road conditions. These inputs are consistent with the standard cross section presented in Table 3.2-1. ESAL inputs use the 90% goods loading case.

	Layer	Thickness (mm)
▶ 1	ABT11 70/100	40
2	ABb16 50/70	50
3	AG22 160/220	65
4	GW-CR (4-6% fines)	80
5	GW-CR (4-6% fines)	420
* 6	4e - Lera	####

Figure 4.6-1: ERAPave layer input showing the pavement structure used in the simulation

4.6.1 ERAPave Pavement Performance Results: Heavy Vehicle

Rutting Results

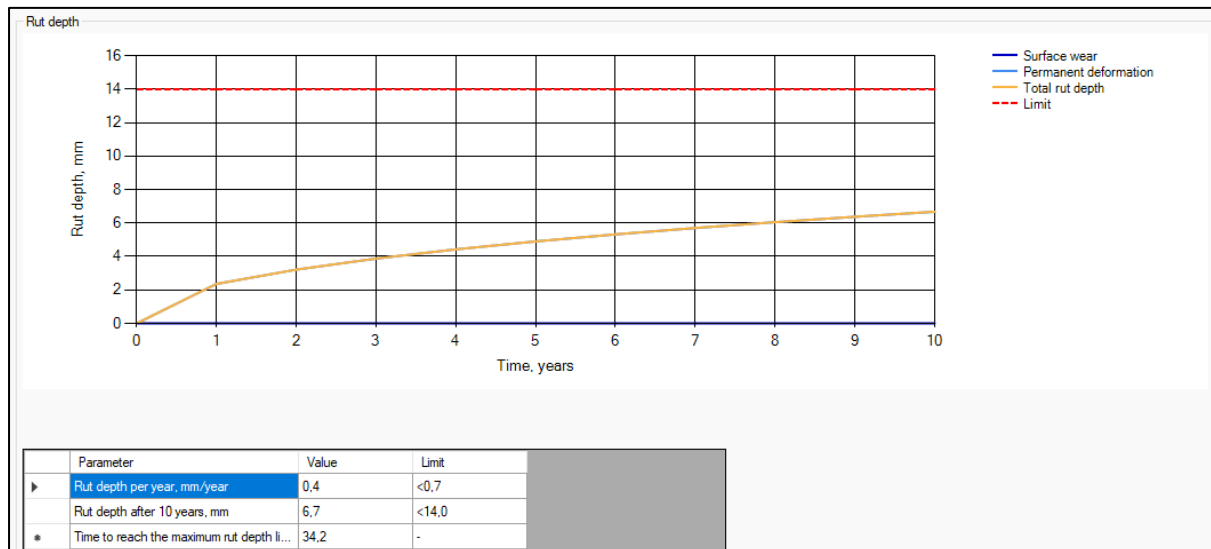


Figure 4.6-2: Rutting Estimated under EV Loading

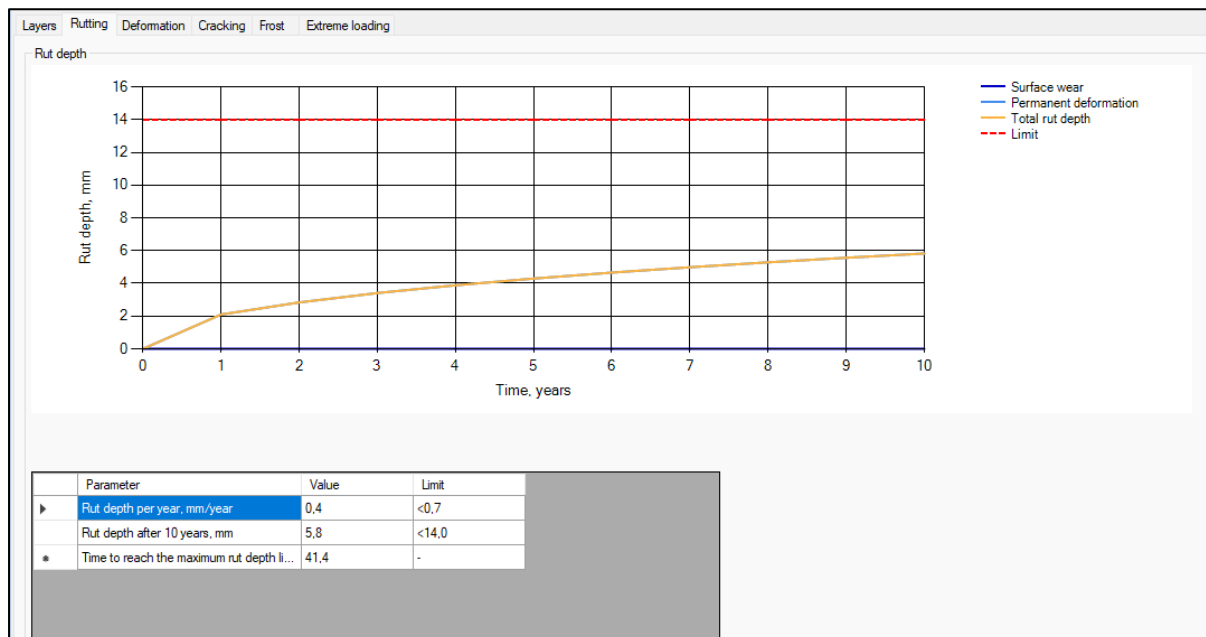


Figure 4.6-3: Rutting Estimated under Diesel Vehicle Loading

The ERAPave results show that, after 10 years the EV pavement is 15% deeper and the 14 mm serviceability limit is reached 7.2 years earlier (34.2 vs 41.4 years). This indicates that if diesel vehicle is replaced by EV vehicles maintenance will be needed approximately 7 years sooner than the roads for diesel traffic. This is a direct maintenance cost increase.

Permanent deformation by layers

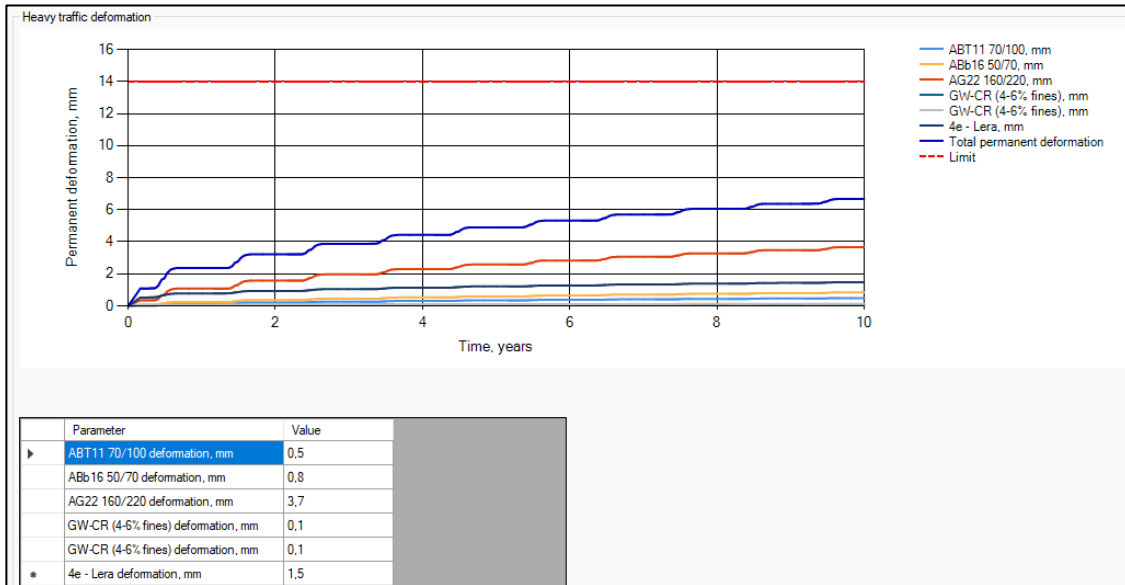


Figure 4.6-4: Permanent Deformation by Layer under EV Loading

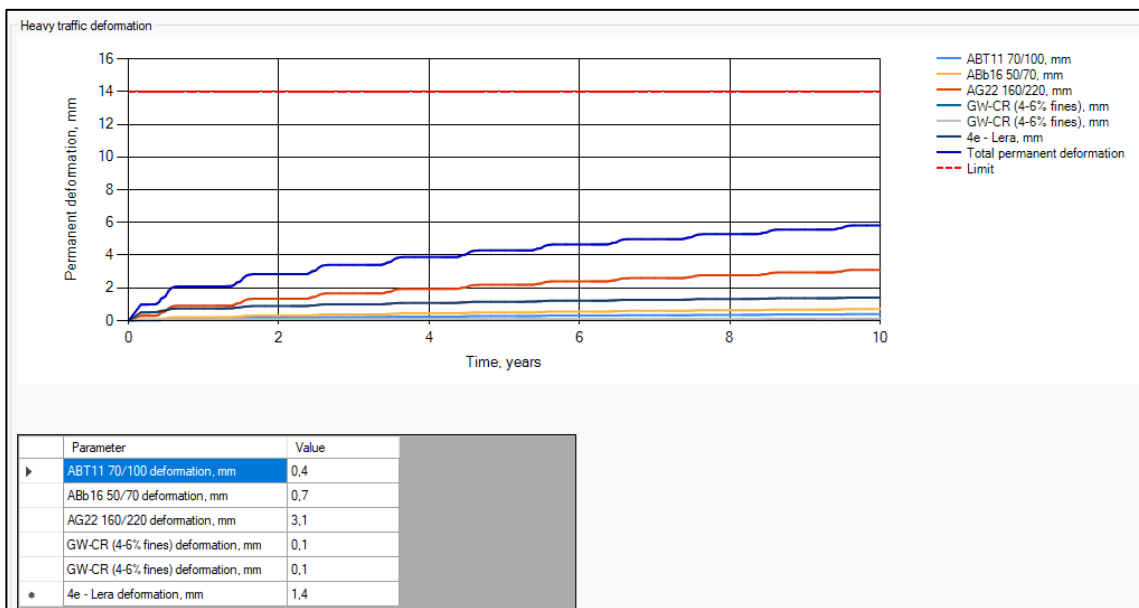


Figure 4.6-5: Permanent Deformation by Layer under Diesel Vehicle Loading

The AG22 asphalt road base is the most affected layer by the EV loading, showing 19% more deformation (3.7 mm vs 3.1 mm). This is structurally significant because the AG22 layer sits at the bottom of the asphalt layer, it is where the maximum tensile strain occurs and where fatigue cracking initiates. The near zero deformation increase in both GW-CR granular

layers. From this result it can be interpreted as rather than a full depth rebuild, asphalt layer reinforcement can reduce the deformation at a great means.

Fatigue Cracking

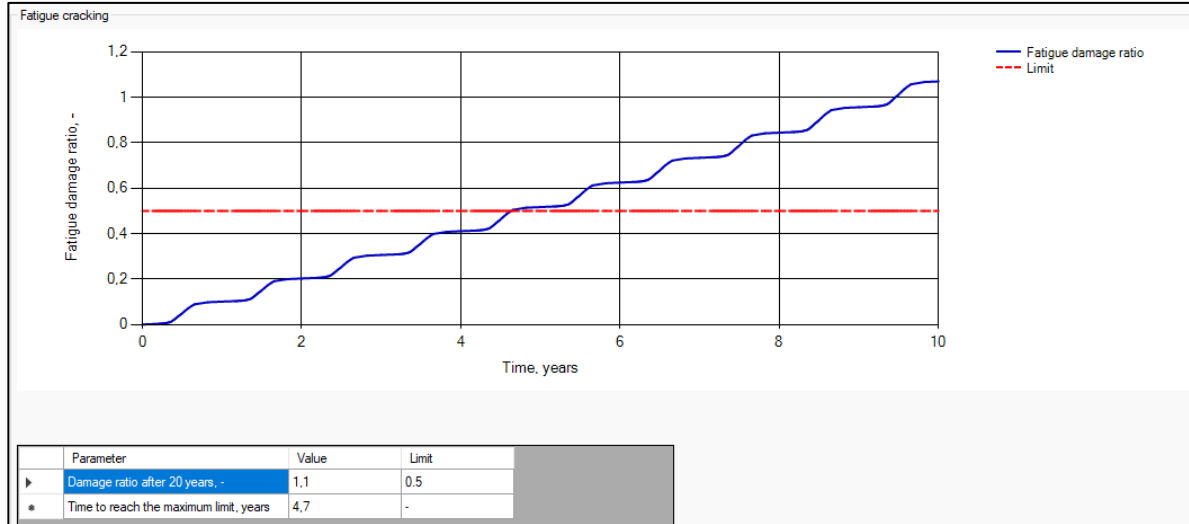


Figure 4.6-6: Fatigue Cracking Caused by EV Loading

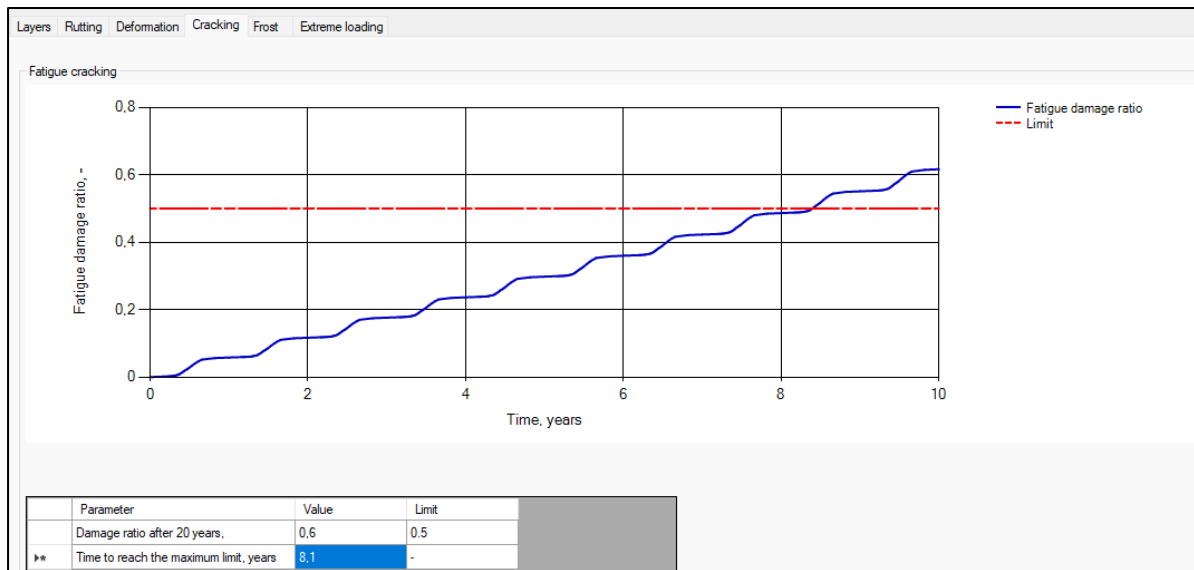


Figure 4.6-7: Fatigue Cracking Caused by Diesel Vehicle Loading

Fatigue cracking represents the most critical distress mode identified in this study. Under EV loading, the structural fatigue limit is reached at 4.7 years, compared to 8.1 years under diesel loading, a reduction of 3.4 years. Notably, both values fall well within a standard pavement maintenance cycle, which raises serious concerns about the adequacy of current pavement designs for routes carrying heavy electric freight vehicles. The fatigue damage ratio at year 10

stands at 1.1 for the EV and 0.6 for the diesel, indicating that fatigue damage accumulates at twice the rate under EV loading. This accelerated deterioration is attributed to the higher axle loads imposed by the battery mass of the EV, which increases tensile strain at the base of the asphalt layers, the location where bottom up fatigue cracking initiates. These findings suggest that existing pavement structures, dimensioned for conventional diesel traffic, may reach structural failure prematurely when subjected to regular heavy EV loading, necessitating a revision of current design and maintenance frameworks.

Table 4.6-1: Summary of ERAPave Result

	Parameter	EV	Diesel	Limit	Key Finding
Rutting	Rut depth (mm)	6.7	5.8	< 14.0	EV 15% deeper
	Time to 14 mm limit (yr)	34.2	41.4		EV 7.2 yr sooner, earlier resurfacing needed
Deformation	AG22 road base (mm)	3.7	3.1		EV +19% in critical structural layer
Fatigue Cracking	Damage ratio	1.10	0.60	< 0.50	Both exceed limit, EV severely beyond
	Time to structural limit (yr)	4.7	8.1		MOST CRITICAL: EV fails 3.4 yr sooner.

4.7 Potential Solutions for EV

The existing pavement structure is insufficient for sustained heavy EV freight loading. Fatigue cracking governs the failure sequence and the structural threshold is breached considerably earlier than under diesel traffic. Applying diesel calibrated maintenance schedules to EV freight routes is therefore insufficient.

A road subjected to regular heavy EV freight traffic will demand structural investigation and probable rehabilitation within a short period of opening or resurfacing. Moreover, EV freight corridors will require resurfacing approximately earlier than the diesel vehicle, which will increase the maintenance expenditure.

One potential long term solution can be to increase thickness of the critical layer. How, changing layer thickness can effect the result is shown in next section.

4.7.1 : Increase layer thickness

In this section layer thickness has been increased for different layers. The additional asphalt depth increases the distance to the pavement neutral axis directly reducing tensile strain at the base of the AC package where fatigue initiates. The new layer thickness and the results from ERAPave are presented in the following table and figures.

Table 4.7-1: ERAPave layer thickness input with increased thickness

Layer	Current (mm)	Proposed (mm)	Comments
ABT11 70/100 (wearing course)	40	55	+15 mm increases total AC thickness directly reducing bottom tensile strain via Ch factor in MEPDG fatigue model
ABb16 50/70 (binder course)	50	65	+15 mm on the thickest AC layer has high structural leverage; binder course carries largest share of bending stress
AG22 160/220 (AC road base)	65	75	+10 mm adds depth to the AC package further pushing the neutral axis and reducing tensile strain magnitude
GW-CR unbound base	80	80	Unchanged
GW-CR subbase	420	420	Unchanged

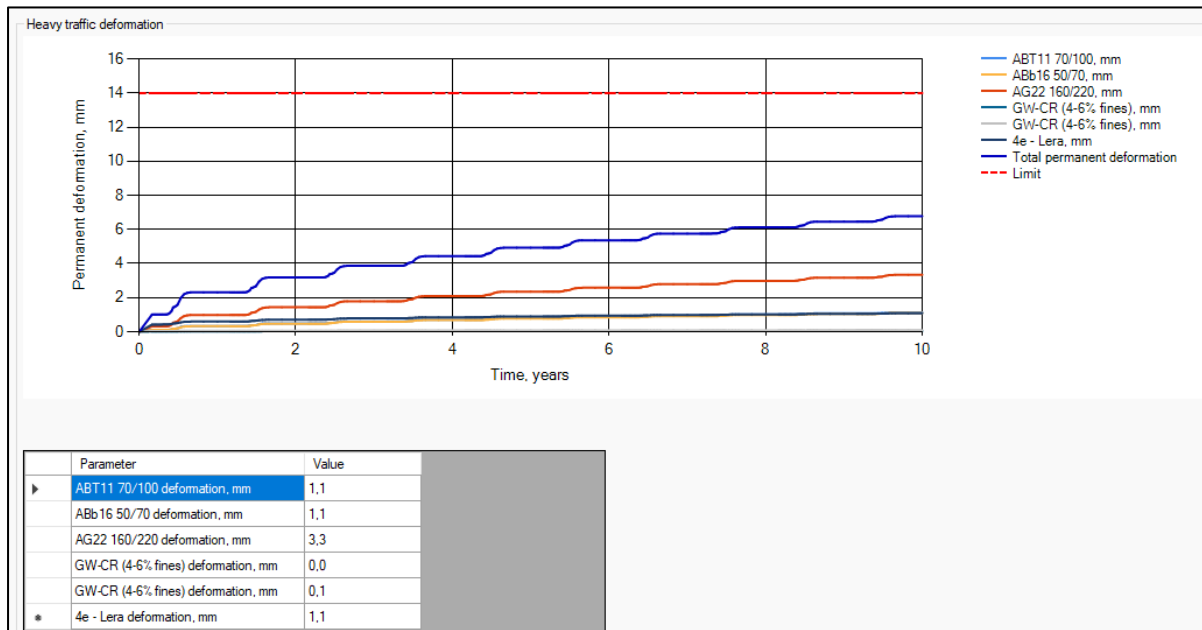


Figure 4.7-1: Permanent Deformation by Layer under EV Loading after Structural Improvement

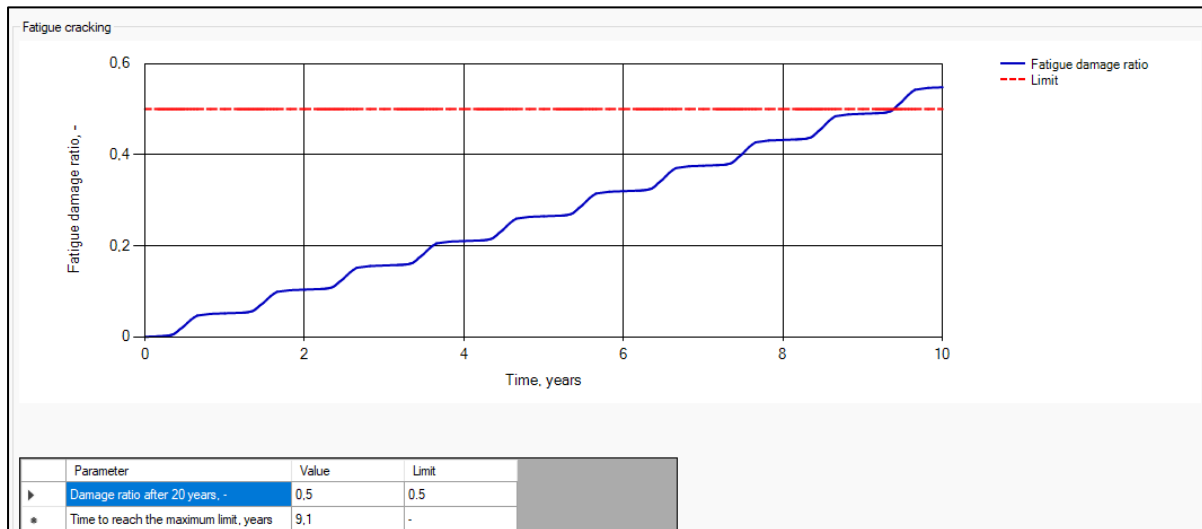


Figure 4.7-2: Fatigue Cracking Caused by EV Loading after Structural Improvement

This solution is highly effective for fatigue cracking. The damage ratio after 20 years drops from 1.1 to 0.5, precisely at the permissible limit, a reduction of 55%. Moreover, the time to reach the fatigue threshold extends from 4.7 to 9.1 years, nearly doubling the serviceable life before structural intervention is warranted. However, implementing this solution comes with additional costs, which will be discussed in the following section.

4.8 Cost difference

In the previous section, it has been discussed that, rutting increases the frequency of the work for maintenance, thus increase the total cost. For improving fatigue cracking, most effective solution can be the increase of layer thickness. In this case, the cost is also will be increased.

To estimate this cost, unit prices are assumed in this analysis. These values are indicative and are not drawn from any published reference or price database. They are used solely to illustrate the cost difference between the baseline and the proposed structure. The assumed unit cost data and calculations are presented in the tables below.

Table 4.8-1: Asphalt mixture cost per mm

Code	Typical layer(s)	Cost per 1 mm·m ² (SEK)
ABS	Surface / top (heavy traffic)	1.92
ABT	Surface / top	1.68
ABb	Binder course	1.68
ABu	Asphalt base	1.68
AG	Surface / binder on low med traffic	1.56

Table 4.8-2: Unbound granular materials cost per mm

Code	Typical use (layer)	Cost per 1 mm·m ² (SEK)
CR (Crushed Rock)	Granular base / subbase	0.50
CG (Crushed Gravel)	Granular base	0.50
GW / GP / GWM (well/poorly graded gravel, moraine)	Subbase / frost layer	0.46
NG (Natural Gravel)	Subbase / local fills	0.44

Table 4.8-3: Layer by layer cost calculation (base vs proposed structure (per m²))

Layer	Rate (SEK/mm ·m ²)	Base Layer (mm)	Proposed layer (mm)	Base layer cost (SEK/ m ²)	Proposed layer cost (SEK/m ²)	Additional cost (SEK/m ²)	Increase (%)
ABT11 70/100	1.68	40	55	67.20	92.40	25.20	37.5%
ABb16 50/70	1.68	50	65	84.00	109.20	25.20	30.0%
AG22 160/220	1.56	65	75	101.40	117.00	15.60	15.4%
GW-CR	0.46	80	80	36.80	36.80	0.00	
GW-CR	0.46	420	420	193.20	193.20	0.00	
TOTAL				482.60	548.60	66.00	13.7%

The additional cost under amounts is 66.00 SEK/m², representing a 13.7% increase over the baseline structure cost of 482.60 SEK/m². This increase stems solely from the three asphalt concrete layers, the granular layers remain unchanged. Within the AC package, the wearing and binder courses each contribute 25.20 SEK/m² and the road base adds 15.60 SEK/m².

Chapter 5: Conclusions

This study quantified how battery electric heavy trucks and passenger cars differ from their diesel and petrol counterparts in axle loading and what those differences mean for flexible pavement performance under Swedish road conditions. The analysis drew on manufacturer specifications for a matched vehicle pair, LEF and ESAL calculations under the European 100 kN reference axle and mechanistic empirical simulation in ERAPave, calibrated for Nordic seasonal conditions.

Regarding RQ1, the Volvo FM EV carries a steering axle load of 6,010 kg, compared to 4,995 kg for the diesel, a fixed increment of 1,015 kg attributable to the front mounted battery pack. This asymmetry is independent of payload. Because of the fourth power relationship between axle load and pavement damage, this concentrated front axle mass translates into a substantially elevated damage potential at the steering axle under all operating conditions.

Regarding RQ2, the EV generates consistently higher ESALs than the diesel across all loading scenarios. The ESAL ratio peaks at 2.92 under the empty condition and narrows to 1.69 at 90% goods loading, but remains above unity throughout. ERAPave simulations at 90% loading confirm that fatigue cracking governs the failure sequence. The structural fatigue threshold is reached at 4.7 years under EV loading, against 8.1 years for diesel, a reduction of 3.4 years. The fatigue damage ratio at year 10 stands at 1.10 for the EV and 0.60 for the diesel, against a permissible limit of 0.50. Rutting progresses at a secondary rate, with EV rut depth 15% deeper after 10 years and the 14 mm serviceability limit reached 7.2 years earlier. For the passenger car pair, the EV generates 1.72 times more ESALs than its petrol counterpart. The per vehicle increment is almost equal to the lowest ratio of heavy truck, but accumulates across millions of daily passes as Sweden's passenger fleet electrifies.

Regarding RQ3, increasing the three asphalt bound layers by a combined 40 mm to 15 mm on the wearing course, 15 mm on the binder course and 10 mm on the road base, reduces the fatigue damage ratio from 1.10 to 0.50 and extends the time to fatigue threshold from 4.7 to 9.1 years. Because additional deformation concentrates entirely within the AC package,

granular layer modifications are not required. The construction cost premium for this adaptation is 66.00 SEK/m², representing a 13.7% increase over the baseline structure.

The overarching conclusion is that the standard Swedish national road cross section is structurally insufficient for sustained heavy EV freight loading. Diesel calibrated design standards and maintenance schedules, applied without revision to routes carrying electric heavy trucks, will result in premature fatigue failure, shortened service intervals and increasing maintenance expenditure. The findings support a revision of pavement design guidance for designated EV freight corridors, incorporating the axle load characteristics of commercially available European electric trucks and Nordic climate conditions. Future work should extend this analysis to thinner municipal road networks, where structural vulnerability to overloading is greater and validate the specification based loading assumptions against field measured axle loads from in service electric truck.

References

- Afridi, M. A. (n.d.). *Municipal street pavement maintenance and management practices in Sweden*.
- Afridi, M. A., Erlingsson, S., & Sjögren, L. (2023). Municipal street maintenance challenges and management practices in Sweden. *Frontiers in Built Environment*, 9, 1205235. <https://doi.org/10.3389/fbuil.2023.1205235>
- Afridi, M. A., Erlingsson, S., Sjögren, L., & Englund, C. (2025). Predicting Pavement Condition Index Using an ML Approach for a Municipal Street Network. *Journal of Transportation Engineering, Part B: Pavements*, 151(2), 04025025. <https://doi.org/10.1061/JPEODX.PVENG-1568>
- Ahmed, A., & Erlingsson, S. (n.d.). *ERAPave PP/VegDim User's Guide*.
- Arizona State University, Jayme, A., Hernandez, J., Marquette University, Al-Qadi, I., University of Illinois Urbana-Champaign, Cardenas, J., University of Illinois Urbana-Champaign, Hafeez, M., University of Illinois Urbana-Champaign, Villamil, W., & University of Illinois Urbana-Champaign. (2025). *Impact of Heavy Commercial Electric Vehicles on Flexible Pavements*. Illinois Center for Transportation. <https://doi.org/10.36501/0197-9191/25-003>
- Chua, B., & Nepal, K. (2025). The Effect of Electric Heavy Vehicles on Flexible Pavements in Australia: A Review. *American Journal of Civil Engineering*, 13(6), 373–390. <https://doi.org/10.11648/j.ajce.20251306.15>
- Engholm, A., Frölander, S., Johansson, M., Kristofersson, F., & Kristoffersson, I. (2025). Impacts of electric and driverless heavy-duty trucks on the future decarbonized freight transport system: Analyzing techno-economic uncertainty using exploratory modeling

- and analysis. *Transportation Research Part A: Policy and Practice*, 199, 104576. <https://doi.org/10.1016/j.tra.2025.104576>
- EV Charging Index 2025: Expert insights from Scandinavia*. (n.d.). Roland Berger. Retrieved May 1, 2026, from <https://www.rolandberger.com/en/Insights/Publications/EV-Charging-Index-2025-Expert-insights-from-Scandinavia.html>
- Fares, M. Y., Albdour, A., & Lanotte, M. (2024). Evaluation of potential electric vehicles load-induced damage on flexible pavements. *Transportation Research Part D: Transport and Environment*, 136, 104475. <https://doi.org/10.1016/j.trd.2024.104475>
- Fares, M. Y., & Lanotte, M. (n.d.). *Electric Vehicles Induced Damage on Flexible Pavement in Arid Climates*.
- Gkyrtis, K. (2025). The Impact of Weight Distribution in Heavy Battery Electric Vehicles on Pavement Performance: A Preliminary Study. *World Electric Vehicle Journal*, 16(9), 520. <https://doi.org/10.3390/wevj16090520>
- Gregor, E. (n.d.). *Sweden's climate action strategy*.
- Hägg, J. (2025, April 29). *Potholes: Sweden, Europe, USA*. <https://www.niradynamics.com/latest/potholes-sweden-europe-usa>
- John Harvey, A. S. (2020). *Effects of Increased Weights of Alternative Fuel Trucks on Pavement and Bridges*. <https://doi.org/10.7922/G27M066V>
- Liimatainen, H., Van Vliet, O., & Aplyn, D. (2019). The potential of electric trucks – An international commodity-level analysis. *Applied Energy*, 236, 804–814. <https://doi.org/10.1016/j.apenergy.2018.12.017>
- Mattinzioli, T., Butt, A. A., & Harvey, J. (2023). Literature review on pavements and electric vehicle interaction: A research roadmap. *Transportation Research Part D: Transport and Environment*, 122, 103886. <https://doi.org/10.1016/j.trd.2023.103886>
- Meßmer, M., Moura, A., Lopes, R. B., Bublies, S., & Svejkský, S. (2025). Data-driven

- insights into truck utilisation challenges in freight logistics. *Research in Transportation Business & Management*, 60, 101373. <https://doi.org/10.1016/j.rtbm.2025.101373>
- NVDB på karta. (n.d.). Retrieved May 20, 2026, from <https://nvdbpakarta.trafikverket.se/>
- Okte, E., & Al-Qadi, I. L. (2022). Impact of Autonomous and Human-Driven Trucks on Flexible Pavement Design. *Transportation Research Record: Journal of the Transportation Research Board*, 2676(7), 144–160. <https://doi.org/10.1177/03611981221077083>
- Statistics Sweden. (2023). *Körsträckor 1999-2022*. <https://www.trafa.se/globalassets/statistik/vagtrafik/korstrackor/2022/korstrackor-1999-2022---2023-09-22.pdf>
- Sweden: 35% BEV market share in 2024 | *European Alternative Fuels Observatory*. (n.d.). Retrieved May 11, 2026, from <https://alternative-fuels-observatory.ec.europa.eu/general-information/news/sweden-35-bev-market-share-2024>
- Sweden proposes the 2026-2037 National Infrastructure Plan – *Ministero degli Affari Esteri e della Cooperazione Internazionale*. (n.d.). Retrieved May 1, 2026, from https://www.esteri.it/en/sala_stampa/archivionotizie/approfondimenti/2024/02/svezia-proposta-di-piano-nazionale-delle-infrastrutture-per-il-periodo-2026-2037/
- Sweden reaches 15% EV car fleet in 2025 | *European Alternative Fuels Observatory*. (n.d.). Retrieved May 11, 2026, from <https://alternative-fuels-observatory.ec.europa.eu/general-information/news/sweden-reaches-15-ev-car-fleet-2025>
- Sweden's Climate Act and Climate Policy Framework. (n.d.). Retrieved May 1, 2026, from <https://www.naturvardsverket.se/en/topics/climate-transition/sveriges-klimatarbete/swedens-climate-act-and-climate-policy-framework/>

- Sweden's EV Market in January 2025: 14.4% YoY increase | European Alternative Fuels Observatory. (n.d.-a). Retrieved May 1, 2026, from <https://alternative-fuels-observatory.ec.europa.eu/general-information/news/swedens-ev-market-january-2025-144-yoy-increase>
- Volvo trucks. (2025). *Volvo Trucks biggest in electric trucks in Europe and North America*. <https://www.volvotrucks.com/en-en/news-stories/press-releases/2025/mar/volvo-trucks-biggest-in-electric-trucks-in-europe-and-north-amer.html>
- Wikström, P. (2024). *Prognos för godstransporter 2045: Trafikverkets Basprognoser 2024* [Elektronisk resurs]. Trafikverket.
- Zhou, Q., Ramakrishnan, A., Fakhreddine, M., Okte, E., & Al-Qadi, I. L. (2024). Impacts of heavy-duty electric trucks on flexible pavements. *International Journal of Pavement Engineering*, 25(1), 2361087. <https://doi.org/10.1080/10298436.2024.2361087>



CHALMERS
UNIVERSITY OF TECHNOLOGY